Measurement of soot mass and PAHs during the pyrolysis of C$_2$-C$_4$ alcohols at high temperatures

Zuhaib Ali Khan*, Paul Hellier, Nicos Ladommatos

Department of Mechanical Engineering, University College London, Torrington Place,

London, WC1E 7JE, UK

*Corresponding author

Email: zuhaib.khan.17@ucl.ac.uk (Zuhaib Khan)

Abstract

Particulate matter (PM) is emitted from a range of combustion sources, can vary greatly in properties, and is able to penetrate deep into the human lungs, conveying carcinogenic PAHs present on the particle surface. Alcohol based biofuels have been shown to potentially reduce PM emissions when displacing fossil fuels. To improve understanding of the influence of fuel bound oxygen on and the relative toxicity of PM, this paper investigates quantitatively the soot mass and PAHs produced from the pyrolysis of ethanol, 1-propanol, 2-propanol,1-butanol, and 2-butanol in a laminar flow reactor. The pyrolysis of alcohol fuels and collection of soot-bound and gas-phase PAH was carried out between 1323-1623 K at a fixed carbon atom concentration in nitrogen. Accelerated solvent extraction (ASE) was used to extract soot bound PAH and gaseous species captured on XAD resin, with speciation and quantification of PAHs undertaken using GCMS. Of the primary alcohols, the highest and lowest masses of soot were observed for 1-butanol and ethanol respectively, while secondary alcohols generated more soot mass than corresponding primary alcohols. An effect of hydroxyl group position on the total PAH distribution in the gas and particulate-bound phases was observed within the temperature range of 1323 to 1423 K. At 1323 K, 1-propanol produced approximately three times more particle phase (PP) PAH concentration than 2-propanol. Among the fuels tested, 1-propanol produced the highest level of carcinogenic PAHs at 1323 K, while for all C$_3$ and C$_4$ fuels the toxicity equivalence factor decreased with increasing pyrolysis temperature.

1   Highlights:

Longer chain alcohols produced more soot mass during pyrolysis

Secondary alcohols generated more soot mass than corresponding primary alcohols

1-propanol pyrolysis at 1323 K saw the highest levels of toxic PAH

2   Keywords: Alcohol fuel, Pyrolysis, Soot, PAHs, Toxicity

3   Introduction

The continuing detrimental effects of particulate emissions from different engineering combustion systems on health and atmospheric air quality, despite continuous strict global particle emissions legislation, necessitates further examination of their formation and toxicity. Poly aromatic hydrocarbons (PAHs), found adsorbed onto the surface of soot particles, are the principal source of this toxicity [1]. The connection between poly aromatic hydrocarbons and soot formation is reasonably well-understood, with PAHs considered to be the principal soot precursors. Following the formation of single aromatic rings, the rings grow via a number of mechanisms into larger species and eventually form into soot particles. Fine particles pose a greater risk to human health as they can be inhaled and carry PAHs deep into the lungs [2]. The United States Environmental Protective Agencies (US EPA) has listed 16 potentially toxic PAHs which are cited worldwide. Out of these 16 PAHs, benzo[A]pyrene is considered the most toxic [3]; its link with human lung cancer has been established [4], and is therefore among the most studied PAHs [5]. The 16 priority US EPA PAHs investigated in this study, with abbreviations, is shown in Table 1.

Alcohol based biofuels are considered to be potential sustainable alternative fuels, either on their own or as blending components, because they can be obtained from a variety of potentially sustainable materials which can be sourced worldwide [6]. Several experimental and numerical studies have been carried out to investigate the combustion characteristic of alcohol biofuels including ethanol, propanol, and butanol, where the addition of alcohol fuels to fossil fuels reduced the emissions of polyaromatic hydrocarbons and particulates matter. Among all the alcohol fuels, ethanol is widely considered as a liquid alternative fuel [7,8]. Ethanol and its blends with other fuels have been previously studied in different combustion systems, such as tube reactors and flames [9–18]. From these studies, it can be concluded that the addition of ethanol to fossil fuel suppressed the sooting tendency and PAHs formation. Esarte et al., 2011, 2012 studied the effect of the addition of ethanol to acetylene pyrolysis in a flow tube reactor and reported that the addition of ethanol promotes the formation of carbon monoxide and methane, which in turn prevents much of the fuel carbon forming soot and PAHs.

Propanol and butanol have been studied in flow reactors[11,17,19], shock tubes [20–25], flames [26–33], and engine [34–38]; these works focus on enhancing the understanding of the gas phase processes during the combustion process. However, some studies have investigated the effect of butanol isomers on the formation of PAHs and soot propensity[13,33,39]. For example, Vikeri et al., 2017 studied the effect of 1-butanol, 2-butanol, iso-butanol, and tert-butanol on the formation of PAHs and soot in a pyrolysis tubular flow reactor at a temperature

range of 1273 K -1473 K and found that the soot mass increased with increasing β H-atoms due to the ease of unimolecular decomposition at these sites. They also found that the total PAHs concentration decreased with an increase of temperature from 1273 K - 1473 K with the highest concentration of PAHs formed at 1273 K regardless of the isomers examined.

Table 1:16 priority PAHs and their abbreviation and TEF Value classified by US EPA [41,42]

PAHs	PAHs abbreviation	Molecular mass (g/mol)	Empirical formula	Carcinogenic group	TEF value	Number of rings
Naphthalene	NPH	128	$C_{10}H_8$	D	0.001	2
Acenaphthylene	ACY	152	$C_{12}H_8$	D	0.001	3
Acenaphthene	CAN	154	$C_{12}H_{10}$	NA	0.001	3
Fluorene	FLU	166	$C_{13}H_{10}$	D	0.001	3
Phenanthrene	PHN	178	$C_{14}H_{10}$	D	0.001	3
Anthracene	ATR	178	$C_{14}H_{10}$	D	0.01	3
Fluoranthene	FLT	202	$C_{16}H_{10}$	D	0.001	4
Pyrene	PYR	202	$C_{16}H_{10}$	NA	0.001	4
Benzo[a]anthracene	B[a]A	228	$C_{18}H_{12}$	B2	0.1	4
Chrysene	CHR	228	$C_{18}H_{12}$	B2	0.01	4
Benzo[b]fluoranthene	B[b]F	252	$C_{20}H_{12}$	B2	0.1	5
Benzo[k]fluoranthene	B[k]F	252	$C_{20}H_{12}$	B2	0.1	5
Benzo[a]pyrene	B[a]P	252	$C_{20}H_{12}$	D	1	5
Indeno[1.2.3-cd]pyrene	I[123-cd]P	276	$C_{22}H_{12}$	B2	0.1	6
Dibenz[a,h]anthracene	D[ah]A	278	$C_{22}H_{14}$	B2	1	6
Benzo[g,h,i]perylene	B[ghi]P	276	$C_{22}H_{12}$	B2	0.01	5

* B2 group 'possible carcinogenic to human', while D group 'as unclassifiable to carcinogenicity' NA- Not available.

Nonetheless, the details of soot and growth of PAHs from the pyrolysis of propanol and butanol isomers that can be drawn from the current literature is limited, and the influence of alcohol carbon chain length and hydroxyl group position on the gas-phase and particle-phase PAHs and their toxicity are still not well understood. Further, understanding of links between specific alcohol isomers and individual PAHs growth mechanisms remain incomplete. Therefore, in order to improve understanding of the influence of alcohol fuel molecular structure on soot and PAHs formation and their relative toxicity, a homologous series of C_2 to C_4 alcohol fuels have been investigated and reported in this paper. The results show the influence of alcohol composition, including chain length, C/O ratio and hydroxyl group position, on soot and PAHs formation, and estimated toxicity, in a pyrolytic environment.

The particulates were generated from the pyrolysis of alcohol fuels in a laminar flow reactor. C_2 to C_4 alcohols were entrained in nitrogen and were pyrolysed at fixed concentration of 10,000 ppm on carbon atoms basis, at a temperature range of 1323 to 1623 K under oxygen free conditions. The soot produced from the pyrolysis of the test fuels was collected from the exit of the reactor, and the gaseous PAHs at the exit of the reactor were also collected on resin. Both the soot-borne and resin-borne PAHs were then extracted from the samples using accelerated solvent extractor (ASE). This was followed by identification and quantification of the extracted PAHs using gas chromatography coupled with mass spectroscopy (GCMS). The oxygen free pyrolysis and the temperatures range used in the experiments resemble roughly the conditions at the core of diesel engine sprays during the premixed and early diffusion stages of combustion. The above literature review is summarised in Table 2.

Table 2: Summary of previous experimental studies investigating soot and PAHs from short-chain alcohols.

Reference	Alcohols investigated	Reactor or device used	Measured properties	Diagnostic technique
Norton and Dryer, 1990 [17]	Ethanol, Propanol and Butanol	Flow reactor	Species profile	GC
Alexiou and Williams, 1996 [9]	Ethanol	Shock tube	Soot	Spectra-Physics laser
Inal and Senkan, 2002 [43]	Ethanol	laminar premixed flame	Species profile	GCMS
Wu et al., 2006 [15]	Ethanol	laminar premixed flame	Soot	Laser-induced incandescence
McEnally and Pfefferle, 2007 [14]	Ethanol	nonpremixed flame	Benzene and soot	Photography
Böhm and Braun-Unkhoff, 2008 [16]	Ethanol	Shock tube	Soot	He-Ne laser beam
Esarte et al., 2009 [12]	Ethanol	Flow reactor	CO, CO_2, soot	FTIR, GC (TCD+FID)
Esarte et al., 2011 [10]	Ethanol	quartz reactor	Soot and their reactivity	BET,TEM
Esarte et al., 2012 [13]	Ethanol	flow reactor	soot and gas products	GC (TCD+FID)
Viteri et al., 2019 [39]	Ethanol	tubular quartz reactor of	PAHs and gas products	GC (TCD+FID), GCMS
Li et al., 2019 [19]	Propanol	Flow reactor	laminar burning velocity	(SVUV-PIMS)
Wang and Cadman, 1998 [20]	Propanol	Shock tube	Soot and PAHs	HPLC, MS
Moss et al., 2008 [21]	Butanol isomers	Shock tube	ignition delay	Pressure
Johnson et al., 2009 [22]	Propanol and Butanol	Shock tube	ignition delay	Pressure
Heufer et al., 2011 [23]	n-Butanol	Shock tube	ignition delay	Pressure
Stranic et al., 2012 [24]	Butanol isomers	Shock tube	ignition delay	Pressure
Yang et al., 2016 [25]	Propanol	Shock tube	ignition delay	Pressure
Wang and Frenklach, 1997 [44]	Butanol isomers	nonpremixed flame	Species profile	PMS
Yang et al., 2007 [27]	Butanol isomers	Laminar premixed flame	Intermdiate species	MBPMS
Li et al., 2008 [28]	Propanol	low-pressure premixed flame	Species profile	Tunable synchrotron photoionization
Kasper et al., 2009 [29]	Propanol isomer	premixed flat flame	intermediate species	EI and VUV-PMBMS
Frassoldati et al., 2010 [30]	Propanol isomer	non-premixed flames and	intermediate products	GC
Hansen et al., 2011 [31]	n-Butanol	low-pressure premixed flame	mole fraction profile	MBMS
Camacho, Lieb and Wang, 2013 [32]	n-Butanol and i-Butanol	Flame	soot size distribution	PSDF
Singh and Sung, 2016 [33]	Butanol isomers	non-premixed flame	PAHs	Laser-induced fluorescence (PLIF)
Popuri and Bata, 1993 [36]	Butanol	Engine	Anti-knock	Oscilloscope
Zervas et al., 2002 [35]	2-propanol	Engine	Exhaust emissions	GC-FID
Lü et al., 2006 [34]	2-propanol	HCCI Engines	Exhaust emissions	Gas analyser
Rakopoulos et al., 2010 [37]	Butanol	Bus engine	Exhaust emissions	Gas analyser
Yao et al., 2010 [38]	n-Butanol	HD diesel engine	Exhaut emissions	MEXA-7100DEGR exhaust analyzer

Experimental methodology

3.1 Experimental setup and conditions

3.1.1 Sampling generation

The experiments on the alcohol fuels were carried out in a high temperature flow reactor facility described in detail previously [45–48], therefore only a brief description is given here. The reactor tube was 1440 mm long with an inside diameter of 104 mm and it was vertically positioned and heated electrically. The pyrolysis of the C_2 to C_4 alcohol fuels was carried out at a fixed concentration of 10,000 ppm on a carbon atom basis in a heated nitrogen stream flowing through the reactor tube, at a temperature range of 1323 to 1623 K at atmospheric pressure. Oxygen-free nitrogen procured from BOC was used as the carrier gas with a fixed flow rate of 20 l/min (STP conditions) and was metered through a mass flow controller. The soot and gaseous products generated by the pyrolysis of fuels were collected at the exit of the tube reactor on a 70 mm glass microfibre filter paper (chosen as it should not contain any PAH prior to soot sampling) and XAD-2 resin respectively. Fig 1 shows in schematic form the tube reactor used for all experiments, with gaseous and liquid fuel supply lines and sample paths for soot and XAD-2 resin collection.
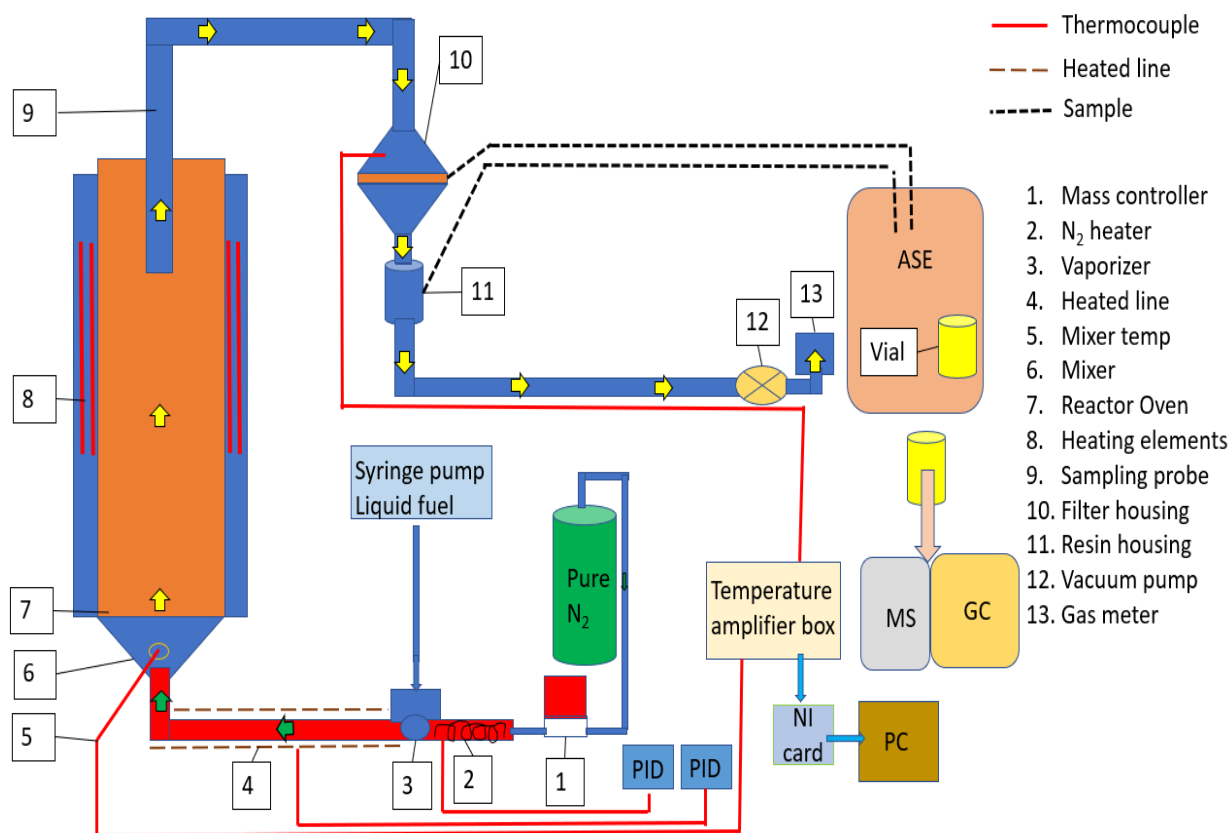
Fig 1:Schematic diagram of the tube reactor facility.

The accuracy (including linearity and based on actual calibration supplied by the manufacturer) of the Bronkhorst mass flow controller was ±0.5% Rd plus ±0.1% FS, while the uncertainly in readings from the k-type thermocouples utilised was ± 1 ^{0}C. All soot masses were weighed on a mass balance of 1 μ g resolution.

The longitudinal temperature profile used in this work has been previously reported [49]. For this study the gas residence time, which is the ratio of tube reactor volume/gas flow rate at a set temperature was t(s) = 4479/T. Table 3 shows the soot yield ((Conc. soot (mg/m^3) /(carbon inlet (mg)/N$_2$ inlet (m^3)))*100) and the residence time for each fuel and temperature tested.

Table 3: Alcohol soot yield (% wt/wt) at varying residence time and temperature.

Temperature (K)	Residence Time (s)	Ethanol %	1-Propanol %	2-Propanol %	1-Butanol %	2-Butanol %
1323	3.4	0.0	0.04	0.17	0.06	0.58
1423	3.1	0.3	2.88	5.27	4.91	5.94
1523	2.9	2.8	7.62	11.50	9.43	11.06
1623	2.8	1.3	5.55	9.24	7.28	9.53

3.1.2 PAHs extraction

The particle and gas-phase PAHs were extracted from the soot collected on the filter paper and on the XAD-2 resin using a Thermofisher Scientific Dinox-150 accelerated solvent extractor (ASE) using dichloromethane (DCM) as the solvent. DCM has a lower boiling point (40 ^{0}C) compared to all PAHs (218-536 ^{0}C) and can be easily evaporated during subsequent concentrations of the extracted PAHs for GC analysis. DCM has been used previously by many researchers for PAH extraction[45,50]. The method used for the extraction can be found in the supplementary data, Table S1. For each soot and resin sample, the ASE extraction was repeated three times and a total of 60 ml of extraction was generated from the three extractions.

3.1.3 PAHs concentration

The 60 ml extract was first concentrated to 15 ml by gently blowing pure nitrogen across the surface of the extraction vial, which was placed on a heated block; the temperature of the block was maintained at 40°C by a PID controller. The 15 ml extraction was then transferred to a 15 ml graduated glass tube and subsequently concentrated further to 1 ml.

3.1.4 PAHs analysis

The 1 ml concentrated samples were analysed using Gas chromatography coupled with mass spectrometry with a Restek Rxi-17Sil MS (Fused silica, 30 m* 250 µm*0.25 µm) column. Pure helium was used as a carrier gas with a flow of 2 ml/min. A GC automatic liquid sampler (ALS) was used with an injection volume of 1 µL in a split-

less mode. The GC oven was initially heated to a temperature of 65 ^{0}C and held for 0.5 min, then ramped up as follows: to 220 ^{0}C at a rate of 15 ^{0}C/min and held for 1 min; to 330 ^{0}C at a rate of 4 ^{0}C/min and held for 0.5 min; post-run at 339 ^{0}C for 5 min. Total run time for each sample was 39.83 minutes and the transfer line was maintained at a temperature of 290 ^{0}C. The MS used was a single quadrupole in electronic ions (EI) mode, with MS source and quad temperatures of 230 ^{0}C and 150 ^{0}C respectively.

For quantification of PAHs, an external standard mix was used containing the 16 EPA priority PAH, detailed in Table 1. This was procured from Sigma Aldrich at a 2000 µg/ml concentration diluted in dichloromethane (DCM). As the PAHs on the particulate and in a gaseous phase were present at a wide range of concentrations, the external standard was first diluted from 2000 to 50 ppm and then further serially diluted to six calibration standards. For dilution, high purity DCM was procured from Sigma Aldrich. An internal standard mix of 2000 µg/ml concentration diluted in dichloromethane was also procured from Sigma Aldrich. The internal standard mix was further diluted to the middle concentration of the calibration standards and was added to all the samples and calibration standards vials for PAHs quantification as recommended by EPA Method TO-3A. EPA Method TO-3A for the internal standard was adopted for PAH quantification where different PAH of the 16 were assigned to one or more of the specific deuterated PAH within the internal standard. The internal standard mix contained five deuterated PAHs and more details can be found in supplementary data, Table S2. Fig 2 shows a sample chromatogram of the 20 ppm calibration standard measured in selected ion mode. The numbered peaks shown in Fig 2 are the 16 priority PAHs e.g. number 1 is Naphthalene while number 16 is Benzo (g,h, i) perylene, while the five smaller peaks apparent in the chromatogram, labelled a to e, are the deuterated PAH utilised as internal standards.
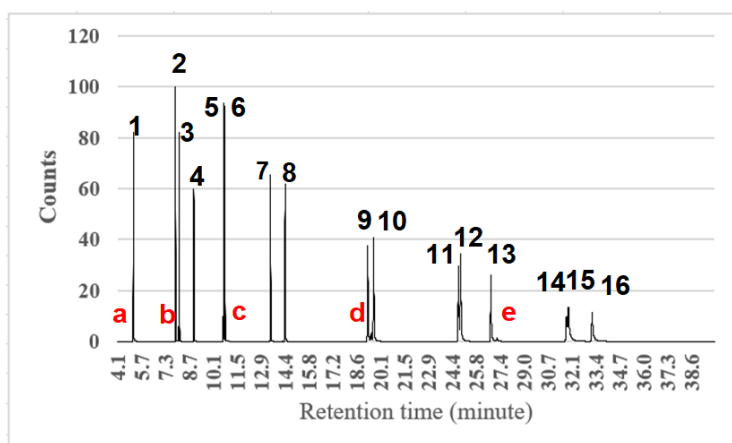
Fig 2: Sample chromatogram of the 20 ppm calibration standard in selected ion mode

3.2   C$_2$-C$_4$ alcohol fuel molecules

Five, 99.6 % certified AR grade, alcohol fuels were sourced from Sigma Aldrich and their properties are shown in Table 4. These fuels consisted of the C$_2$-C$_4$ straight chain alcohol (ethanol, 1-propanol and 1-butanol) and C$_3$-C$_4$ straight chain alcohol isomers (1-propanol,2-propanol and 1-butanol,2-butanol). The C$_4$ branched alkyl chain alcohol isomers (iso-butanol and tert-butanol) were not included as the primary focus of the current study was the impact of the hydroxyl group as opposed to the presence of methyl branching within an alkyl moiety. Fig 3 shows the test fuel molecular structure.

Table 4:Tested C$_2$-C$_4$ alcohol fuels and their properties [51–53]

Fuel	Molecular structure	Carbon to oxygen ratio (C/O)	Molar mass (g/mol)	Density (Kg/m^3) at 25 ^{0}C	Boiling point (^{0}C)	Purity
Ethanol	C$_2$H$_5$OH	2	46.06	789	78	99.9%
1-Propanol	CH$_3$(CH$_2$)$_2$OH	3	60.09	804	97	99.9%
2-Propanol	CH$_3$CH$_2$(OH)CH$_3$	3	60.09	785	83	99.9%
1-Butanol	CH$_3$(CH$_2$)$_3$OH	4	74.11	810	118	99.9%
2-Butanol	CH$_3$CH$_2$CH$_2$(OH)CH$_3$	4	74.11	808	99	99.9%
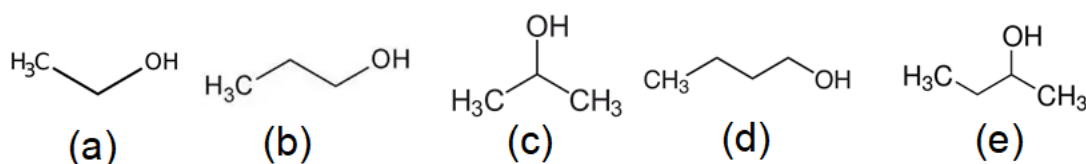
Fig 3: Fuel molecular structure (a) Ethanol, (b)1-Propanol, (c) 2-Propanol, (d) 1-Butanol, and (e) 2-Butanol

Therefore, the following effects of the alcohol fuel molecular structure on the soot propensity and PAHs formation at temperatures between 1323 K and 1623 K were investigated:

Influence of increasing alkyl chain length and hydroxyl group position on soot propensity, and on the amount of gas-phase and particle-borne PAHs, and the estimated toxicity of PAHs.

Possible mechanisms that lead to individual PAH growth from alcohol molecules.

4   Results and discussion

In this section of the paper the experimental results and discussion are presented.

4.1   Fuel effects on soot mass concentration

Fig 4 shows the mass of soot collected from the C_2-C_4 alcohols at a range of temperatures from 1323 K to 1623 K, where the mass of soot collected from the filter was normalised with the volume of gas drawn through the filter. The measurement of soot mass concentration and PAHs from ethanol pyrolysis was repeated 5 times so as to assess the repeatability of experimental analytical processes, and in Fig 4, and throughout, where shown in results figures, the error bars show plus and minus one standard deviation from the mean value, where the mean value is obtained from repeated ethanol pyrolysis. Ethanol was chosen as a reference fuel due to the higher oxygen to carbon ratio relative to the other test fuels and observed a lower mass of soot collected for a constant supply of 10,000 ppmC (Table 3). Apparent from Fig 4 is an increase in soot concentration concurrent in general with an increase in the carbon number of the alcohols, and also with increasing temperature up to 1523 K.
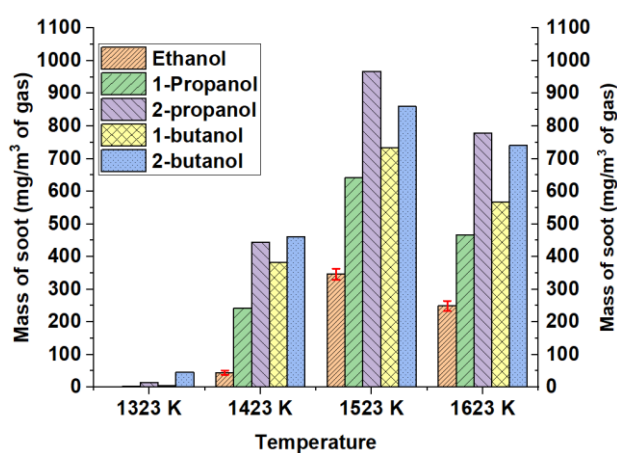
Fig 4: Mass of soot collected of C_2-C_4 alcohols series fuels during pyrolysis at a temperature range of 1323 K to 1623 K normalized per volume of gas.

Fig 4 shows that the mass concentration of soot collected increased with increase of temperature of the tube reactor from 1323 K to 1523 K and subsequently slightly decreased at 1623 K for all the fuels examined. Also apparent in Fig 4, is that the soot mass concentration for all fuels changed significantly from 1323 K to 1423 K, and in future work; however, the exact initiation temperature of elevated soot formation for each fuel was not investigated further in the current work which focused on the relative effects of fuel molecular structure on soot and PAHs formation at consistent temperature conditions. This increase in the mass concentration of soot with rising temperature is consistent with that reported previously in the literature [9,10,54]. It is apparent from Fig 4 that the pyrolysis of the C_3 and C_4 alcohol fuels produced a considerably higher mass of soot in comparison to C_2 alcohol. Increasing the carbon number of C_2-C_4 alcohol fuels increased the mass concentration of soot at all temperatures tested, with 2-propanol an exception at 1523 K and 1623 K producing more mass of soot than 2-

butanol. The pyrolysis of ethanol produced considerably lower soot mass concentrations, in comparison to the C_3 and C_4 alcohols. For instance, at 1523 K ethanol produced 2.8 times less the mass of soot than 2-propanol. At a temperature of 1323 K, ethanol produced no soot and this observation is supported by similar findings by other researchers [10]. The observed increase in soot mass with both alcohol carbon number and C/O ratio is further explored in Section 4.3. It is also evident from Fig 4 that the 2-propanol isomer yielded more soot than 1-propanol at all temperatures tested. For instance, at a temperature of 1523 K 2-propanol produced 1.5 times more soot mass concentration than 1-propanol. This difference in soot mass between the two propanol isomers might be due to the difference in the formation rate of the propargyl radicals (C_3H_3), as reported in the literature [55]. The propargyl radical is considered to be one of the main precursors in the formation of the first aromatic ring [56,57] which is a prerequisite to subsequent PAHs growth and initial soot particle inception. Propargyl radicals also play an important role in the formation of the two-ring species e.g. indene and naphthalene, via phenyl and propargyl, and propargyl and benzyl, reaction sequences [58,59] without first forming a benzene ring. Furthermore, it has also been reported that 2-propanol yields more propene by the four-centre molecular dehydration reaction as compared to 1-propanol; in turn, propene converts readily into propargyl radical leading to a greater yield of soot mass [30]. Considering the C_4 butanol isomers, the position of the hydroxyl group influenced the yield of soot mass, with 2-butanol observed to produce more soot mass than 1-butanol. For example, at 1623 K 2-butanol produced 1.3 times more soot mass concentration as compared to 1-butanol. This trend of high soot mass by 2-butanol could be due to the two butanol isomers having different reaction pathways via the four-centre elimination reaction, both butanols predominantly consumed by H-abstraction [31,40]. The higher sooting tendency of 2-butanol is likely to be due to the higher availability of β H-atom compared with 1-butanol [40]. The consistent production of more soot by 2-butanol relative to 1-butanol is in agreement with similar findings reported in the literature [26,32] and also with the influence of OH position observed in the case of propanol.

In summary, the results in Fig 4 for the C_2 to C_4 alcohol fuels show that an increase in carbon number (and thus also C/O ratio given the pyrolytic conditions) increased the soot mass concentration at all temperatures, except in the case of 2-propanol at 1523 K and 1623 K. Furthermore, a difference can be observed in the conversion of C_3 and C_4 alcohol isomers to soot mass concentration, with secondary alcohols yielding higher soot mass at all temperatures than the corresponding primary alcohols for reasons discussed above.

4.2   Fuel effects on Gas-phase and Particle-phase PAHs

Fig 5 shows the total PAH measured (sum of the 16 US EPA priority PAH speciated) for each of the C2 to C4 alcohols tested.
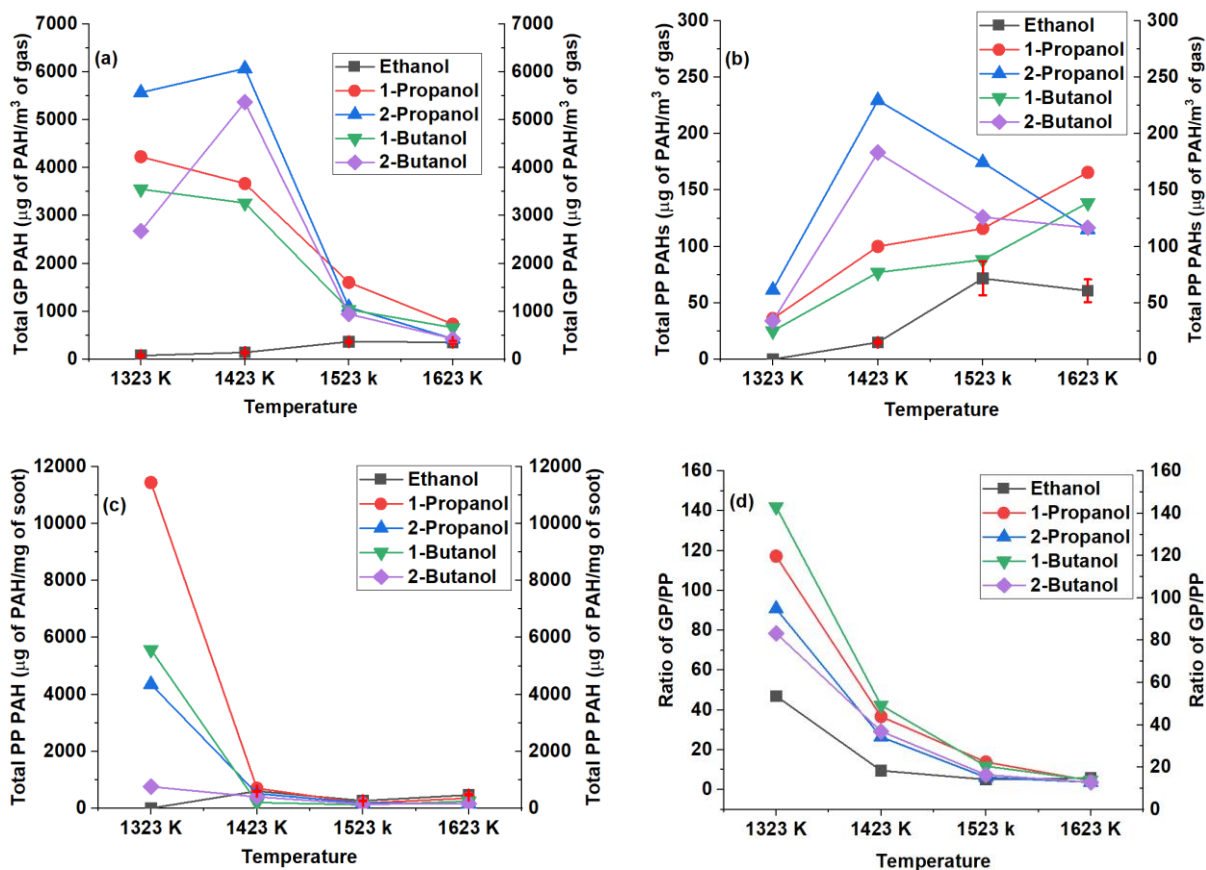
Fig 5: Total PAH produced by straight chain C_2 to C_4 alcohols: (a) Total gas-phase PAH per m^3 of gas,(b) Total particle-phase PAH per m^3 of gas, (c) Total particle-phase PAH per mg of soot (d) Ratio of GP/PP per m^3 of gas. Error bars denote standard deviation for ethanol fuel. Please note the maximum value of the y-axis is significantly lower in fig5b relative to the other sub-figures.

Fig 5a presents the gas-phase (GP) PAH mass concentration extracted from the XAD-2 resin per unit volume of gas drawn through the resin. The concentration of lighter species 2, 3, and some 4 ring PAHs up to pyrene is much greater in the gas phase, however, in this study heavier species were also observed in the gas phase, details can be found in supplementary data, Tables S3 and S4. The high concentration of lighter PAHs in the gas phase is in agreement with previous studies [60]. Fig 5b shows the particulate-phase (PP) PAH that has been extracted from the particulate deposited on the filter paper per unit volume of gas drawn through the filter. Fig 5c shows the particulate-phase PAH extracted but this time normalised with the mass of soot collected on the filter, while Fig 5d is the ratio of PP/GP normalized per volume of gas.

In Fig 5a, the C_3 and C_4 alcohol fuels show decreasing concentrations of gas-phase (GP) PAH with increasing temperature in the range of 1423 K to 1623 K. This is likely to be due to a decrease in the concentration of lighter PAHs (2 and 3 rings) at higher temperatures above 1423 K as shown in

Fig 8. It is likely that the decrease in the GP PAH concentration with increased temperature is the result of increased rates of conversion of GP PAHs to heavier PAHs, and subsequently to soot particles. Ethanol pyrolysis resulted in a significantly lower GP PAH concentration in comparison with that for C_3 and C_4 fuels at all temperatures (Fig 5a), and this may potentially be attributable to the slower formation of intermediate PAH precursors (i.e. acetylene) from ethanol pyrolysis. It is also interesting to note from Fig 5a that pyrolysis of 2-propanol resulted in the highest concentration of GP PAH at all temperatures relative to the primary alcohols tested, despite a shorter carbon chain length and lower carbon to oxygen ratio than 1-butanol. One possible reason might be that the pyrolysis of 2-propanol may produce species including propargyl radical, vinyl acetylene, acetylene, and 1,3 butadiene [28], which are precursors for aromatic ring formation [1,56,61,62] and PAH growth [63], thus increasing the amount of GP PAH.

Fig 5a shows a clear influence at low temperatures (1323 K to 1423 K) of the effect of hydroxyl group position on GP PAH concentration, while at higher temperatures (1523 K to 1623 K) this effect is diminished. A possible explanation for this observation is that at higher temperatures the rates of chemical kinetics are much faster (due to the effective collision of fast-moving particles) [64], with temperature effects thus being dominant compared with any influence of fuel molecular structure.

In Fig 5b, the C_2-C_4 fuels show much lower concentrations of particle phase (PP) PAHs per unit volume of gas than the corresponding concentrations for the gas phase (GP) PAHs shown in Fig 5a. A possible explanation is that some of the particle phase (PP) PAHs condensing onto the particulate surface underwent surface reactions or were incorporated (layered) into the particle [65] and were therefore not extractable by the solvent during the ASE process.

Fig 5c, shows a high PP PAH concentration for the C_3 and C_4 fuels at the lowest pyrolysis temperature of 1323 K, but that this concentration decreased drastically when the temperature rose to 1423 K and it decreased further as the temperature reduced to 1523 K. It is suggested that as the temperature rises the PP PAH condensation process onto the particulate surface results not only in adsorbed PAHs that can be subsequently removed through solvent extraction, but also in the incorporation of PAHs into the soot particle structure which can no longer be removed by solvent extraction [60]. The incorporated PAHs may be contributing to the increased mass of soot with increased in temperature, observed in Fig 4. It is also possible that the decrease in the PP PAHs with increasing temperature is due to a more organised soot micro-texture [66], which makes it less reactive [67] with PAH and thus reducing the amount of adsorbed PP PAHs. The high amount of PP PAHs at 1323 K, might be due to the smaller particle size distribution at 1323 K^0C and relatively large total surface area of soot particle presented

for the condensation of particle-phase PAHs [45]. The slight increase in the PP PAH in the temperature range of 1523 K to 1623 K, suggested that relatively more mass of PP PAHs was deposited on the soot surface, while the amount of soot reduced with further increases in temperature as shown in Fig 4.

Fig 5c, show that the effect of OH position on the PP PAH was greater in the temperature range of 1323 to 1423 K. At 1323 K, 1-propanol produced approximately three times more PP PAH concentration than 2-propanol, and likewise, 1-butanol produced approximately five times more PP PAH than 2-butanol. A possible explanation for the greater mass of PP PAHs for 1-propanol and 1-butanol at 1323 K is that less carbon is being converted into soot mass as shown in Fig 4, hence, more carbon was available for PAHs formation at the lowest temperature.

Fig 5d shows the ratio of GP PAH to PP PAH. It can be seen that at lower temperatures that the level of GP PAH significantly outweighs that of PP PAH, however, at higher temperatures this ratio drops below 20:1 for all fuels, indicating that the relative consumption of GP PAH to PP PAH and soot has accelerated. Interestingly, Fig 5d also shows that the ratio of GP to PP PAH is lower for ethanol relative to the longer chained alcohols at all temperatures, perhaps suggesting that the molecular structure of ethanol inhibits the formation of the initial benzene ring and 2 or 3 ring PAHs but does not detrimentally effect rates of larger PAH formation.

Reconsidering the GP and PP PAH concentrations shown in Fig 5a and 4b the GP PAH concentration for the C_3 and C_4 fuels decreased with increasing temperature, while the PP PAH concentrations were less temperature sensitive. An explanation for these observations might be that the rate of gas-phase GP PAH formation, their growth, and eventual conversion into soot particles was much faster than the rate at which these PAHs condensed onto the soot particle surface, especially since the GP PAHs had considerably lower saturation temperatures than the PP PAHs.

4.3   Effects of carbon to oxygen ratio (C/O) on soot mass, GP and PP PAHs

Fig 6 shows the effect of the alcohol carbon to oxygen ratio on the soot mass, and gas-phase and particle Phase PAHs, each normalized against the carbon to oxygen ratio of each alcohol tested (Table 4). It is apparent from Fig 6a that 2-propanol consistently produces the highest mass of soot at all temperatures except 1323 K, whereas without the normalization a greater mass of soot was produced by 2-butanol at the two lower temperatures tested (Fig 7a). Considering the primary alcohols, it can be seen in Fig 6a that at 1423 K an increase in soot mass with increasing alcohol chain length persists despite normalising of the measured masses (Fig 4) with an increasing C/O ratio (Table 4), with this effect diminishing at higher temperatures.
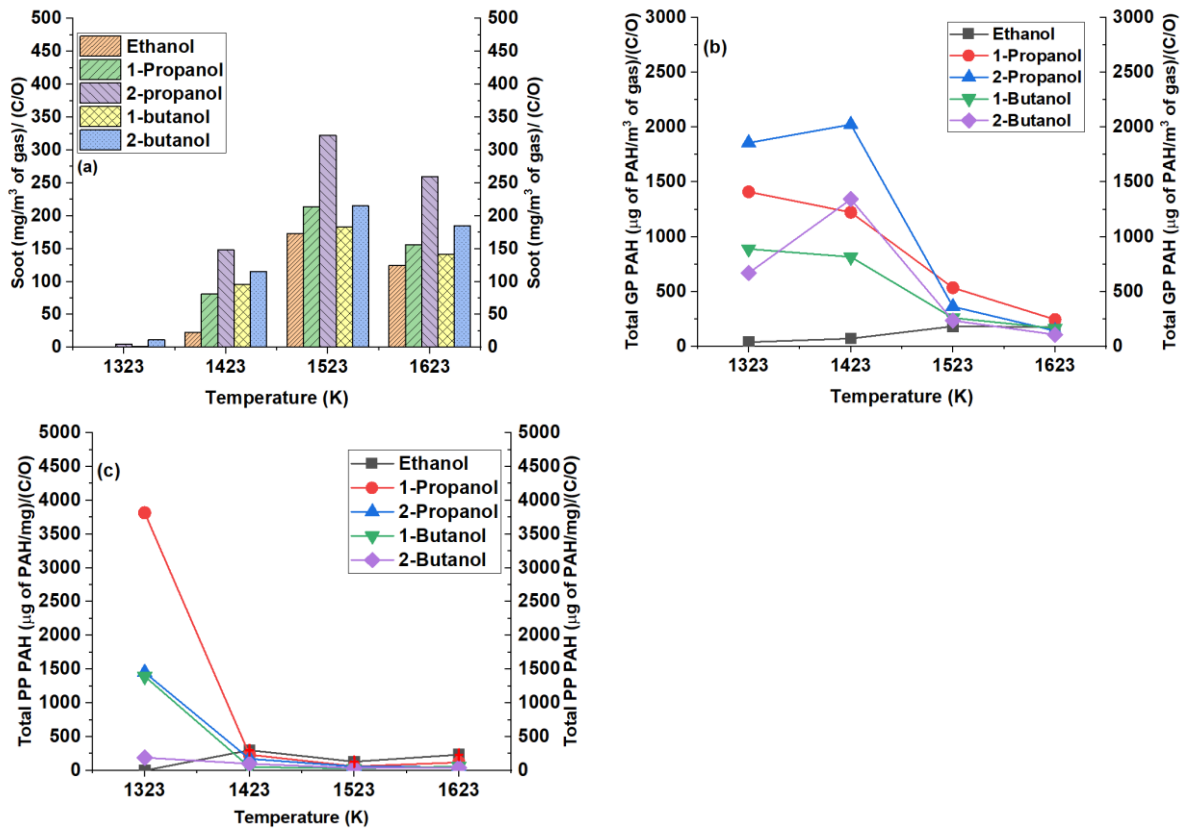
Fig 6: (a) Mass of soot (b) Gas-phase (GP) PAHs and (c) Particle-phase (PP) PAHs collected during the pyrolysis at a temperature range of 1323 K to 1623 K, each normalized against the C/O ratio

Fig 6b shows the total gas-phase PAH (μg of PAH/m^3 of gas) normalized against the carbon to oxygen ratio of each alcohol. The Figure shows that when GP PAH was normalized with C/O ratio, differences in the mass of GP PAH produced by each fuel persisted but decreased in magnitude at the lowest tested temperature of 1323K. In particular, it can be seen that the C/O normalised values of GP PAH for the C_3 and C_4 alcohols are now appreciably lower but still somewhat greater than that displayed by ethanol. At higher temperatures of 1523 K and 1623 K, the effect of carbon to oxygen ratio can be seen to be minimal.

Fig 6c shows the total particle-phase PAH (gas and particle phases, μg of PAH/m^3 of gas) normalized against the carbon to oxygen ratio of each alcohol. Comparing Fig 6c with Fig 5c shows minimal impact on the distribution of PP PAHs when the data for PP PAHs were normalized against the carbon to oxygen ratio. It is interesting to note that the 2-propanol and 1-butanol are brought together at the lowest tested temperature. However, at higher temperatures, above 1423K, there are no effects on the PP PAHs of molecular structure and C/O ratio. These results reflect a significant effect of temperature the PP PAHs.
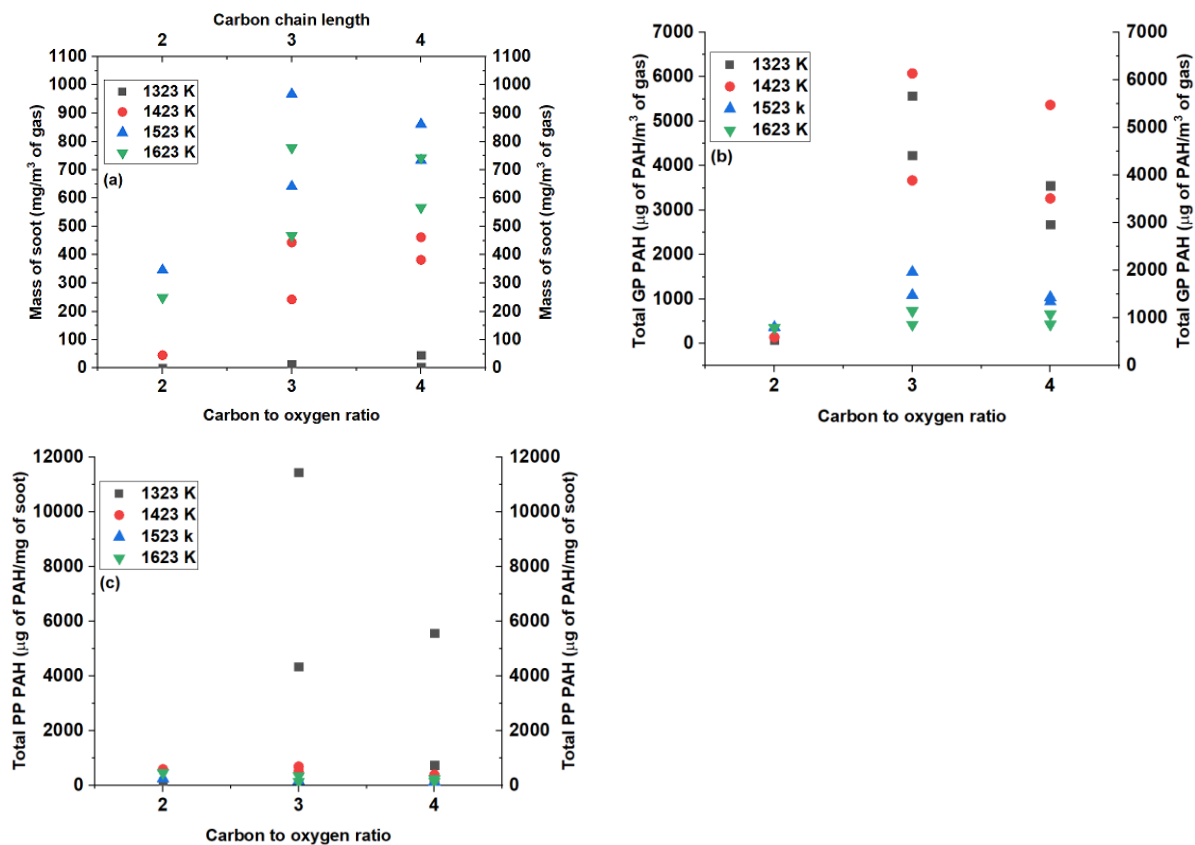
Fig 7: (a) Mass of soot, (b) GP PAHs, and (c) PP PAHs collected during the pyrolysis at a temperature range of 1323 K to 1623 K, each plotted against the C/O ratio

Fig 7a shows the mass of soot (mg/m^3 of gas) plotted against the carbon to oxygen ratio of the alcohol fuel tested. It can be observed from Fig 7a that the soot mass increased with increase in carbon to oxygen ratio, irrespective of fuel molecular structure due to less oxygen per mole of carbon being available; however, 2-propanol, does not follow this trend, as discussed previously in Section 4.1. It is also evident from Fig 7a that at constant C/O ratio the secondary alcohols produced more mass of soot than the corresponding primary alcohols, especially in the case of 2-propanol. However, it should be noted that as the C/O ratio increased, the alcohol carbon chain length also increased.

Fig 7b shows the total gas-phase PAH (μg of PAH/m^3 of gas) plotted against the carbon to oxygen ratio. It can be observed from this Figure a general trend of GP PAHs for all the alcohol fuel molecules to increase up to a C/O ratio of 3 and then slightly decrease at higher ratio. The effect of isomerisation is also evident from Fig 7b.

Fig 7c shows the total particle-phase PAH (μg of PAH/m^3 of gas) plotted against the carbon to oxygen ratio. It can be observed from Fig 7c that PP PAHs increased at the higher C/O ratios, particularly at the lower temperature of 1323K and less so at the higher temperatures.

From the presentation of the above results, it is apparent that there is a relationship between C/O ratio and soot mass, and GP and PP PAHs. It is therefore necessary now to consider possible reasons for this relationship and possible pathways through which this relationship is realised. In this context, however, it should be noted that the oxygen present in the reactor is fuel bound, and it is suggested that it is important to consider whether this oxygen becomes freely available as an oxidizing species or whether it remains carbon-bound. The discussion that follows considers the relationships between C/O and soot mass, GP and PP PAHs in the context of whether the C-O bond is likely to break or not.

Eveleigh et al [68] used similar experimental conditions and the same facilities as for this work to evaluate the conversion rates of fuels (ethanol, 1-propanol, 2-propanol, acetone, and toluene mixed with n-heptane) to particulate matter (PM). Carbon-13 labelling was employed to label specific carbon atoms in the fuel molecule to 13C, which allowed the determination of the contribution of particular fuel carbon atoms to particulate matter by means of isotope ratio mass spectrometry. The technique allowed carbon atoms that were directly connected to the hydroxyl group (OH) and other oxygen bonds to be traced. It was found that the fuel carbon-oxygen bonds remained mostly intact and the greatest contribution to PM mass came from the fuel carbon atoms that were not bonded to oxygen. For example, for ethanol pyrolysis, the methyl carbon contributed 68% to the PM mass thus suggesting that the oxygen mostly might not be freely available to participate in the reaction pathways and, therefore, the influence of fuel-bound oxygen is likely to be lower on PAH and soot formation, compared with that for free molecular oxygen in reactors running with oxidising conditions. Eveleigh et al [68] also found that the carbon atom attached to the OH group of 1-propanol and 2-propanol contributed 16% and 22% of the soot mass, respectively, which might be reflected in the difference in soot mass produced by the isomers stated in Section 4.1.

According to Westbrook et al [69], the C-O bond in various oxygenated molecules survives the fuel-rich ignition intact, suppressing fuel carbon from forming soot precursors and readily producing carbon monoxide. In the context of compression engine Westbrook et al [69], suggests that the strong carbon monoxide bond does not break, and thus the carbon and oxygen atoms remains inaccessible for soot production or to impact on soot formation pathways. The above literature therefore suggests that for small alcohols like ethanol, the likelihood is that the C-O bond would not break most of the time (around 70%), and hence the low mass of soot for ethanol compared with higher alcohols can not only be attributed to a lower C/O ratio, as it is likely that the low mass of soot is also due to a smaller number of carbon atoms available for soot formation [15,70,71]. As with ethanol, it is also likely that in higher alcohols the oxygen atom merely reserves a carbon atom from forming soot. It is likely

therefore that in the case of the alcohols reported in this study, the difference in their C/O ratio may not be the sole or the strongest influence on soot formation, potentially arising from varying ratios of free oxygen and carbon impacting on soot precursor formation pathways; instead, it is likely that increasing fuel carbon chain length has a significant impact in increasing PM mass.

Another possibility, accepting the C-O bond within the alcohols remained intact, is that the higher soot mass, GP and PP PAHs production, for example from propanol relative to ethanol (Figures 4 and 5), might be due to increasing available carbon concentration to form soot (given that all experiments were undertaken on a constant total fuel carbon basis of 10,000 ppm).

Nevertheless, it is suggested that the probability of this having occurred is likely to be low as the results shown in Fig 6a, c, and e are normalized with the C/O ratio but continue to show trends of soot, GP, and PP PAHs concentration with increasing carbon chain length, especially at the lower temperatures at which slower reaction rates can be expected. This suggests that the predominant fuel influence when considering the primary alcohols, at conditions at which PAH formation and conversion to soot is to an extent limited by temperature (for example 1323 K and 1423 K in the current study), is likely the alkyl chain length, rather than the available carbon concentration.

4.4   Effects of alcohol carbon number and OH position on PAH ring distribution

Fig 8 shows the PAH concentration of straight-chain C_2 to C_4 alcohol fuels grouped based on the number of rings.
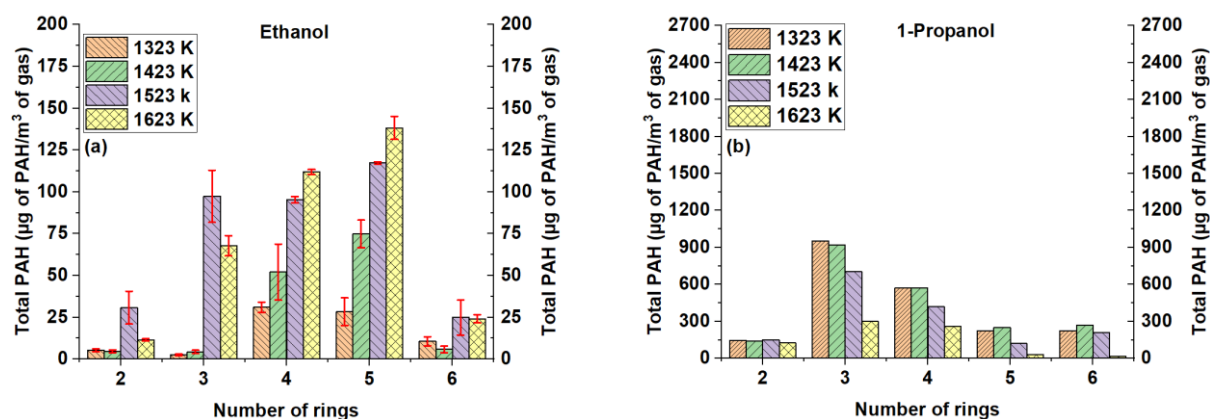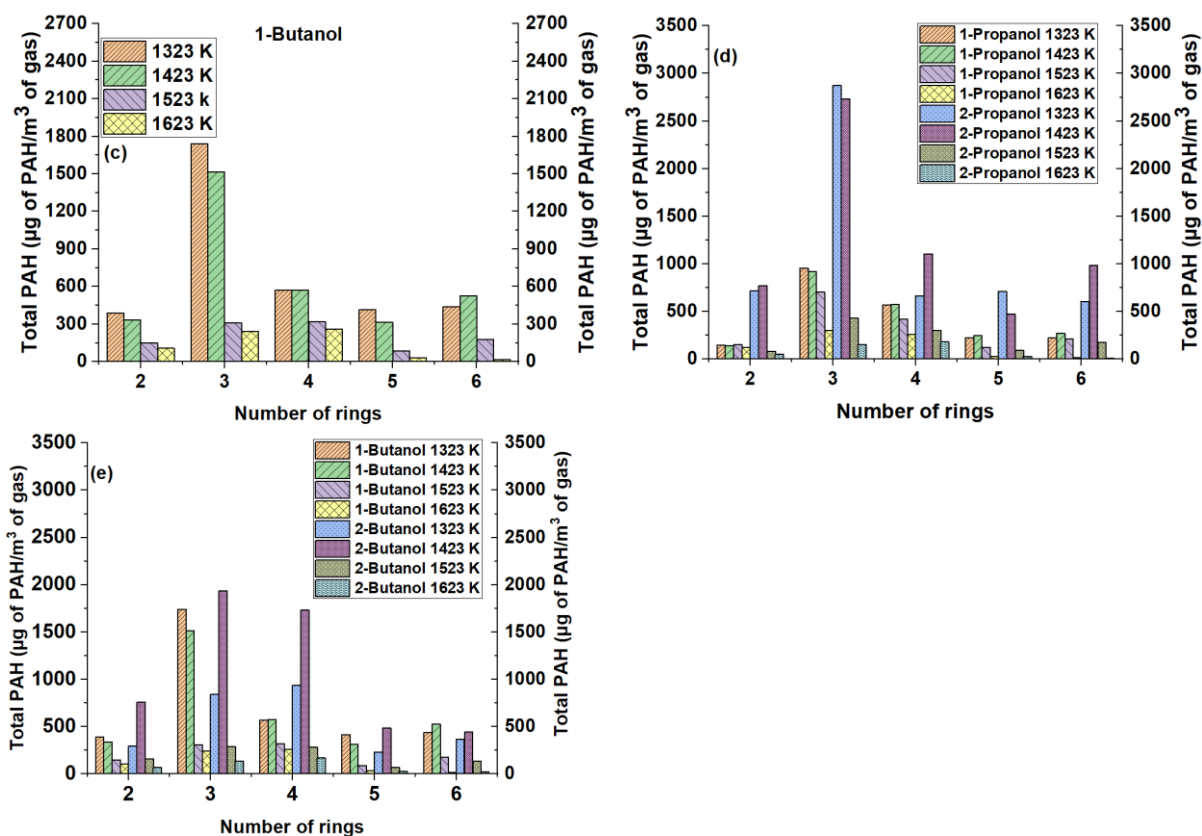
Fig 8: Total PAH (GP + PP) distribution according to the number of rings at four different pyrolysis temperatures (a) Ethanol (b) 1-Propanol (c) 1-Butanol (d) 1-Propanol Vs 2-Propanol (e) 1-Butanol Vs 2-Butanol. Error bars denote standard deviation for ethanol fuel. Please note the maximum value of the y-axis is significantly lower in Fig 8a relative to the other subfigures.

The results presented in Fig 8 provide information on the effect of alcohol size and hydroxyl group position on the growth of PAHs. It can be observed from Fig 8a,b, and c that increasing the alcohol carbon number increased the concentration of PAH of all sizes (as defined by number of rings) at all temperatures.

Fig 8 shows that for C_3 and C_4 alcohol fuels the total PAH concentration (GP + PP) increased from the level for 2 ring species to a maximum level for those with 3 rings, and then decreased progressively in the case of 4, 5, and 6 rings. While in the case of the C_2 alcohol, the PAH concentration increased continuously for 2, 3, 4, and 5 rings and then decreased in the case of 6 rings. It is apparent from Fig 8 that the pyrolysis of C_3 and C_4 alcohols fuels produced considerably higher concentrations of the three ring PAHs (for example, phenanthrene) as compared to 2, 4, 5 or 6 rings. For example, 1-butanol yielded a significant amount of three ring PAH in the temperature range 1323 K and 1423 K and the concentration of three ring decreased with a further rise in temperature. This suggests rapid growth and subsequent conversion of the 3 ring PAHs into soot particles at higher temperatures (Fig 8c). The three ring PAHs play an important role in the growth of 4 to 6 rings PAHs, probably due to more growth sites

at which a new ring could be added rapidly through the HACA mechanism. It can be seen that for C_3 and C_4 fuels the PAH ring concentration increased with increase in temperature from 1323 K to 1423 K and tended to decrease between 1523 K to 1623 K, while a contrary trend can be observed for C_2 alcohol, between 1523 K and 1623 K. Further, the pyrolysis of ethanol yielded higher concentrations of 3,4 and 5 rings at higher temperatures (Fig 8a). From Fig 8b it can be seen that the concentration of two ring PAH remained constant with rising temperatures. Fig 8b and 8c show that the concentration of four ring PAHs were relatively close for the two C_3 and C_4 fuels despite having different carbon chain lengths and C/O ratios. Considering the heavier PAHs (i.e. those with 5 and 6 rings),

Fig 8a,b, and c present that for the C_4 alcohol the abundance of heavier ring PAHs was higher than that for the C_2 and C_3 alcohols. It can be seen that for the C_2 at all temperatures the concentration of 5 ring PAHs was higher than that for the 6 ring PAHs. This difference in the concentration of the 5 and 6 ring PAHs could possibly be ascribed to the difference in the conversion rate of these rings to the soot particles. For the C_3 fuel, the formation rate of 5 ring PAHs and its growth to 6 rings is reasonably close to each other in the temperature range of 1323 to 1423 K.

In Fig 8d and 8e, the effect of OH position on the ring concentration distribution was very evident in the temperature range of 1323 to 1423 K, with 2-propanol producing higher concentrations of all PAH sizes relative to 1-propanol. For example, 2-propanol produced three times more concentration of 3 ring PAHs as compared to 1-propanol in this temperature range. The higher three ring PAH concentration for where the OH group was present on the second carbon of the C_3 alcohol suggests that the conversion of 3 rings PAH to heavier rings PAH was low at lower temperatures [72]. It is clear from Fig 8e that at the lower temperatures of 1323 K and 1423 K there was an effect on the distribution of rings with 1-butanol, with an accumulation of 3 ring PAH at 1323 K, while in the case of 2-butanol a similar effect on 3 and 4 rings is apparent, albeit at a higher temperature of 1423 K.

From the results presented in Fig 8, it can be concluded that the concentration of the 4,5 and 6 rings PAHs for the C_3 and C_4 fuels decreased with the rise of pyrolysis temperature from 1323 to 1623 K, while it increased for ethanol.

4.5   Impact of alcohol carbon number and OH position on individual PAH growth

Fig 9 shows the influence of fuel and temperature on the abundance of various individual PAH, either known to be important species in PAH formation mechanisms or to have high relative toxicity.

(a) Naphthalene

(b) Acenaphthylene

(c) Phenanthrene

(d) Phenanthrene / Acenaphthylene

(e) Pyrene

(f) Benzo[A] Pyrene

(g) Benzo [k] Fluoranthene
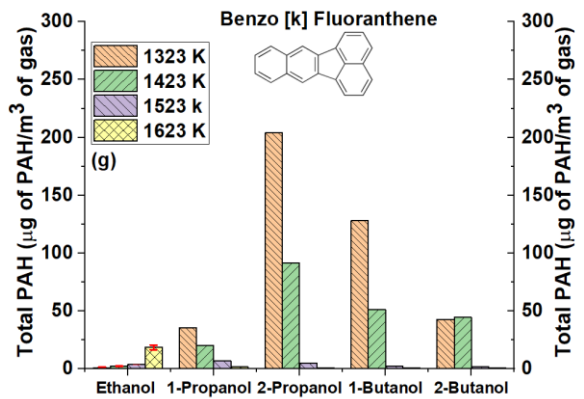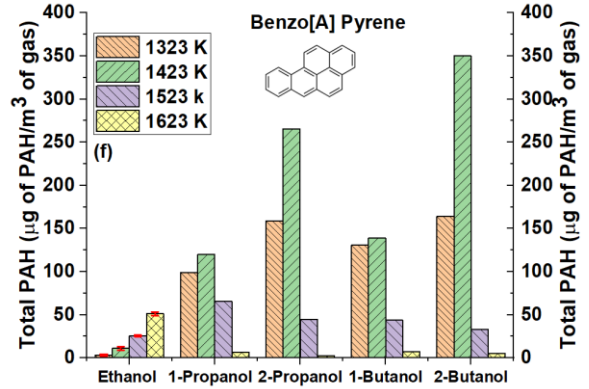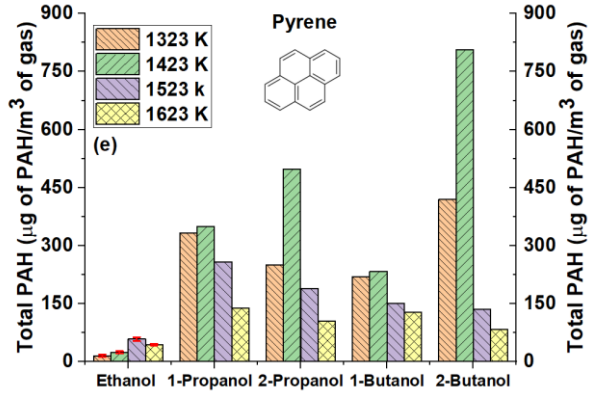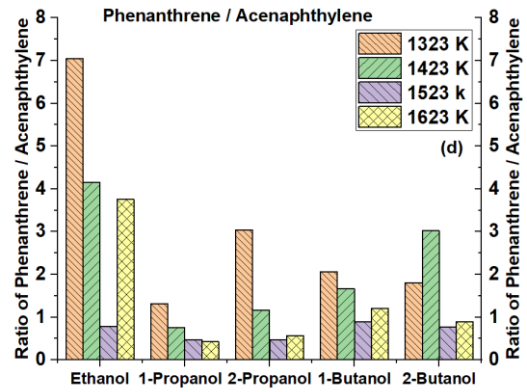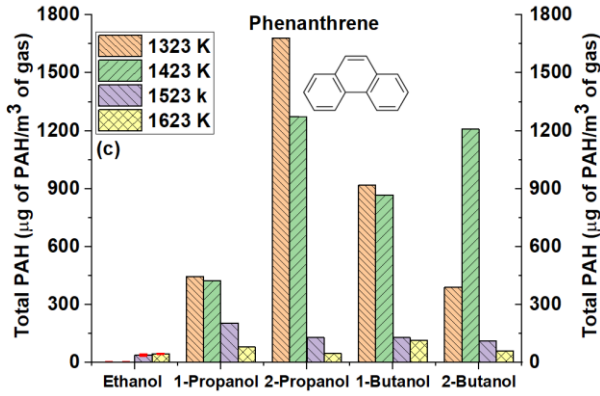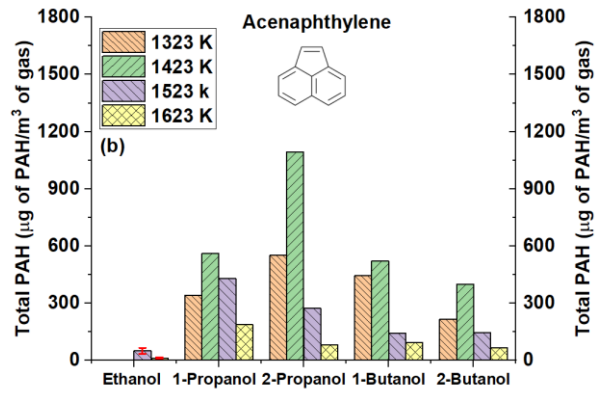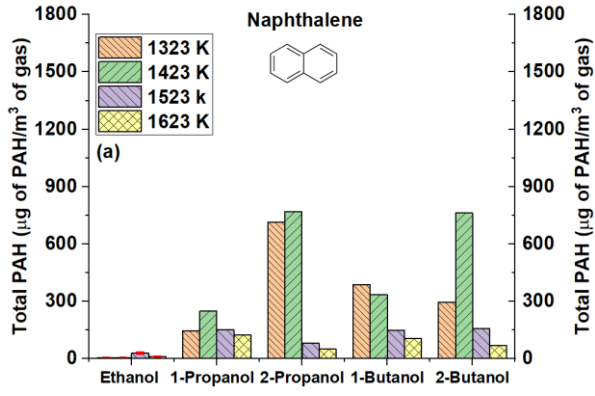
Fig 9: Distribution of Total PAH (GP + PP) during pyrolysis of straight-chain C_2 to C_4 alcohol fuel (a) Naphthalene (b) Acenaphthylene (c) Phenanthrene (d) Ratio of Phenanthrene to Acenaphthylene (e) Pyrene (f) Benzo [A] Pyrene (g) Benzo [K] Fluoranthene. Error bars denote standard deviation for ethanol fuel. Please note the maximum value of the y-axis is relatively significantly lower in Fig 9 e,f, and g.

Fig 9 shows the concentration of Naphthalene (NPH), Acenaphthylene (ACY), Phenanthrene (PHN), Pyrene (PYR), Benzo [A] Pyrene (B[a]P), and Benzo [k] Fluoranthene (B[k]F). These PAHs were selected from the cumulative totals by PAH shown in Fig 8 for further discussion. Fig 9a shows that the concentration of naphthalene increases with an increase in the fuel carbon number in the temperature range of 1323 K to 1423 K, while at higher temperatures the concentration of naphthalene was less effected by the alcohol structure. This might have occurred due to faster conversion with increasing temperature of 2 ring naphthalene to the higher ring PAHs. Ethanol formed its highest concentration of naphthalene at 1523 K while the C_3 and C_4 alcohol formed their highest amounts at lower temperatures. Comparing now the C_3 and C_4 alcohol isomers, Fig 9a shows that at the lower temperature of 1523 K both 2-propanol and 2-butanol produced the highest concentrations of naphthalene, while at both the lowest and highest temperatures of 1323 K and 1623 K there is no such distinct influence of the OH position.

In the case of the C_3 and C_4 alcohols, it has been reported that the propargyl radical pathway for the formation of the first aromatic ring is a dominant pathway for propanol and butanol fuel molecules [33,55], where two propargyl radicals recombined to form a first aromatic ring. After the formation of the first aromatic ring, the benzene ring loses a hydrogen atom, resulting in a phenyl radical which could readily form two-ring naphthalene via the HACA mechanism [62,73]. Although the formation of naphthalene via the HACA mechanism is dominant, it could also be formed by recombining cyclopentadienyl radicals [1]. Once the two-ring naphthalene has been formed, it further grows to three rings acenaphthylene and phenanthrene via the HACA mechanism as shown in Fig 9b and 9c. In Fig 9b, the C_2 fuel produced a low concentration of acenaphthylene as compared to the C_3 and C_4 fuel. From Fig 9b the effect of OH position was notable in the temperature range of 1323 K to 1423 K. For example, at 1323 K, 2-propanol produced almost double the acenaphthylene concentration as compared to 1-propanol, while at 1323 K 1-butanol produced twice the concentration of acenaphthylene as compared to 2-butanol at the same temperature. Fig 9c shows that in the temperature range of 1323 K to 1423 K the concentration of phenanthrene increased with increasing alcohol carbon number. It also shows that 2-propanol produced a higher concentration of phenanthrene at 1323 K and 1423 K than 1-propanol. For example, at 1323 K, 2-propanol produced more than four times the concentration of phenanthrene as compared to 1-propanol. As shown in Fig

9c, the concentration of phenanthrene is high for 1-butanol at 1323 K and 1523 K, while at 1423 K and 1623 K 2-butanol had a higher concentration.

Either the benzenoid phenanthrene or three ring acenaphthylene could grow to form pyrene. From Fig 9d, it can be seen that the concentration of phenanthrene in all the test fuels tended to be higher than that for acenaphthylene at the low temperature range of 1323 to 1423 K and at higher temperatures the contrary trend can be observed. It is therefore suggested that at lower temperatures pyrene growth via phenanthrene dominates through the HACA mechanism, while at higher temperatures pyrene growth is mostly via acenaphthylene. The effect of temperature on the formation of phenanthrene has been reported in a modelling study [74]. The kinetic modelling shows that the pathway of phenanthrene formation from naphthalene could be observed at the lower temperature while the conversion of naphthalene to acenaphthylene became the more favourable pathway beyond 1000 K [74]. Fig 9e shows that all the test fuels produced a substantial amount of pyrene at all temperatures, suggested to be attributable to all the 2 ring and 3 ring PAHs growing via pyrene to form heavier PAH, especially the B2 group (high toxicity group) by the HACA or HAVA mechanisms. Other possible pathways are the PAC (Phenyl addition and cyclization and MAC (methyl addition cyclization) [75,76]. It can be seen from Fig 9f and 9g that in the case of ethanol pyrolysis the concentration of benzo[a] pyrene and benzo[k] fluoranthene increased with increasing temperature while for C_3 and C_4 pyrolysis the concentration of benzo[a] pyrene and benzo[k] fluoranthene decreased with increasing temperature.

4.6   PAH toxicity index

This section evaluates the carcinogenicity of the particulate generated from the test fuels at different temperatures and mainly focuses on the B2 group PAHs due to their high toxicity level. A PAH toxicity index was calculated as the sum of the products of the concentration (Ci) of individual PAHs and their individual toxicity equivalent factor (TEF), as shown in Eq (1). Nisbet and LaGoy (1992) [42] proposed TEFs as found in Table 1, and are widely used to estimate PAH toxicity.

$$\text{Toxicity index} = \sum_{i=1}^{n}(\text{TEFi} * \text{Ci}) \qquad\qquad\qquad (1)$$

The PAH toxicity of the C_2-C_4 alcohols series fuels on a mass of soot basis is shown in Fig 10.
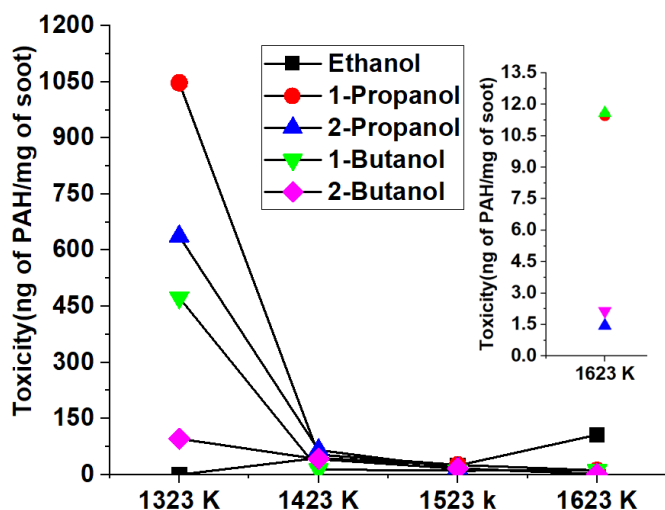
Fig 10: Toxicity of C_2 to C_4 alcohol fuels soot particle per mg of soot.

It can be observed from Fig 10 that at the lowest temperature all the tested fuels exhibit very different toxicity levels, while it is interesting to see how close at the calculated toxicity of particulates from each fuel is at higher temperatures. It is apparent from Fig 10 that 1-propanol had the highest toxicity at 1323 K. For example, the toxicity of 1-propanol at 1323 K was 1.6 times of 2-propanol, 2.2 times that of 1-butanol and 10.8 times that of 2-butanol. The high toxicity of the 1-propanol soot at 1323 K, can be attributed to a relatively high concentration of toxic benzo [a] pyrene condensing onto the soot particles. At this point, it is important to mention that the toxicity level increased 10 times in each PAH growth step from acenaphthylene to benzo [a] anthracene and then to most toxic benzo[a] pyrene. The contribution of other B2 group species to the high toxicity of 1-propanol toxicity can be found as supplementary data, Table S5 and Table S6. The low ring number PAHs possessing low carcinogenicity, and which are classified as group D (low toxicity group), were present at relatively low concentrations on the soot mass collected. The low ring PAHs have high vapour pressure and low boiling point as compared to the B2 group. Therefore, the group D PAHs may have a low condensation rate on the soot surface [54]. 2-propanol has the second highest toxicity at 1323 K while ethanol has the lowest. However, at the highest tested temperature, ethanol has the highest toxicity. It is interesting to note that the primary alcohols are more toxic than the corresponding secondary alcohols at the lowest and highest temperatures.

Finally, it is interesting to note that at the lower temperatures of 1323 to 1423 K the abundance of soot mass is relatively low for all fuels as can be seen in Fig 4, however Fig 10 shows that the toxicity of the extractable PAHs condensing on the soot particles was much higher than it was at temperatures higher than 1423 K. This observation suggests that low temperature combustion systems which are designed for reducing NOx, might at the same time produce more toxic particulates.

5   Conclusions

The influence of carbon number and hydroxyl group position in short chain alcohols on the mass of soot formed and the mass and composition of the 16 priority PAH, listed by the EPA, at pyrolytic conditions was investigated in a high temperature tube reactor. To investigate the effects of alkyl chain length, ethanol, 1-propanol, and 1-butanol were chosen, while the secondary alcohols (2-propanol and 2-butanol) were included to provide insight as to the effects of OH position along a straight alkyl chain. All experiments were conducted at a consistent fuel inlet concentration of 10000 ppm on C_1 basis at a constant residence time of $t(s) = 4479/T$, and at a temperature range from 1323 to 1623 K at ambient pressure.

The results obtained showed that alkyl chain length, C/O ratio, and hydroxyl group position had an impact on the total soot mass produced from the pyrolysis of the alcohol fuels. The soot mass concentration increased with carbon number, which was expected given the increase in the C/O ratio. Normalisation with the alcohol C/O ratio continued to show lower soot mass in the case of ethanol relative to 1-propanol and 1-butanol at 1423 K, suggestive of an influence of alkyl chain length further to that of determining the C/O ratio of each fuel. The secondary alcohols (2-propanol and 2-butanol) consistently generated higher soot mass as compared to primary alcohols (1-propanol and 1-butanol), which is likely attributable to higher rates of decomposition to soot precursors in the case of the secondary alcohols.

Increasing alcohol carbon number had an appreciable impact on the GP PAH concentration, with ethanol pyrolysis resulting in a significantly lower GP PAH concentration relative to that for 1-propanol and 1-butanol at all temperatures; this observation remained valid when normalising with C/O ratio, with the exception of the highest temperature of 1623 K. The effect of hydroxyl group position on the GP and PP concentration was noticeable in the lower temperature range of 1323 to 1423 K. Meanwhile, the concentration of PAH rings increased with an increase in alcohol carbon number. It was found that the pyrolysis of C_3 and C_4 alcohols fuels produced considerably higher concentrations of the three ring PAHs as compared to 2, 4, 5, or 6 rings, with concentrations of the former peaking at 1323 to 1423 K before decreasing appreciably at higher temperatures. This rapid formation and apparent consumption are suggestive of the significant role of the three ring PAH in the subsequent formation of 4 to 6 rings PAHs and soot particles.

It was observed that the pyrene formation pathway was temperature dependant and was mainly dominated by phenanthrene in the temperature range of 1323 K to 1423 K, as indicated by a high ratio of phenanthrene to acenaphthylene for all of the C_2 to C_4 alcohols. However, at higher temperatures of 1523 K to 1623 K pyrene

formation was mainly via the acenaphthylene pathway, with a significant reduction in the ratio of phenanthrene to acenaphthylene observed.

A significant impact of pyrolysis temperature on the calculated toxicity of the particulates was apparent, with a greater abundance of toxic PAHs at low temperature, despite lower temperatures producing smaller soot mass concentrations. The highest toxicity of all the short chain alcohols investigated was observed in the case of 1-propanol at 1323 K, attributable to a relative concentration of benzo[a]pyrene. At the highest temperature of 1623 K, differences in particulate toxicity arising from changes in fuel composition were less apparent, with the highest level exhibited by ethanol.

The presented results showed that there are significant effects of fuel molecular structure on the formation of soot and PAHs, and thus potential implications for air quality and public health in the development of future alcohol based fuels. However, to better understand the influence of the OH group on the decomposition reaction pathways it is recommended that further investigations determine fuel effects on the abundance of smaller hydrocarbons intermediate and precursor species, such as acetylene, propyne, 1,3 butadiene, and benzene, towards mitigating these impacts through fuel design and optimisation of combustion processes.

6   Acknowledgment

7   References

[1]   Richter H, Howard JB. Formation of polycyclic aromatic hydrocarbons and their growth to soot-a review of chemical reaction pathways. Prog Energy Combust Sci 2000;26:565–608. https://doi.org/10.1016/S0360-1285(00)00009-5.

[2]   Allen JO, Dookeran NM, Smith KA, Sarofim AF, Lafleur AL. Measurement of Polycyclic Aromatic Hydrocarbons Associated with Size-Segregated Atmospheric Aerosols in Massachusetts. Environ Sci Technol 1996;30:1023–31. https://doi.org/10.1021/es950517o.

[3]   Levin W, Wood AW, Wislocki PG, Kapitulnik J, Yagi H, Jerina DM, et al. Carcinogenicity on Mouse Skin of Benzo-Ring Derivatives of Benzo (a) pyrene. Cancer Res 1977;37:3356–61. https://doi.org/Published September 1977.

[4]   Mikhail F, Denissenko, Pao A, Tang M. Preferential Formation of Benzo [a] pyrene Adducts at Lung Cancer Mutational Hotspots in P53. Science (80-) 1996;274:430–2.

https://doi.org/10.1126/science.274.5286.430.

[5]   Collins JF, Brown JP, Alexeeff G V, Salmon AG. Potency Equivalency Factors for Some Polycyclic

        Aromatic Hydrocarbons and Polycyclic Aromatic Hydrocarbon Derivatives 1. Regul Toxicol Pharmacol

        1998;28:45–54. https://doi.org/https://doi.org/10.1006/rtph.1998.1235.

[6]   Jess A. What might be the energy demand and energy mix to reconcile the world ' s pursuit of welfare

        and happiness with the necessity to preserve the integrity of the biosphere ? Energy Policy

        2010;38:4663–78. https://doi.org/10.1016/j.enpol.2010.04.026.

[7]   Kumar S, Singh N, Prasad R. Anhydrous ethanol : A renewable source of energy. Renew Sustain

        Energy Rev 2010;14:1830–44. https://doi.org/10.1016/j.rser.2010.03.015.

[8]   Niven RK. Ethanol in gasoline : environmental impacts and sustainability review article. Renew Sustain

        Energy Rev 2005;9:535–55. https://doi.org/10.1016/j.rser.2004.06.003.

[9]   Alexiou A, Williams A. Soot Formation in Shock-Tube Pyrolysis of Toluene , Toluene-

        Methanol,Toluene-Ethanol, and Toluene-Oxygen Mixtures. Combust Flame 1996;104:51–65.

        https://doi.org/https://doi.org/10.1016/0010-2180(95)00004-6.

[10]   Esarte C, Bilbao R, Alzueta MU, Peg M, Ruiz MP. Pyrolysis of Ethanol : Gas and Soot Products

        Formed. Ind Eng Chem Res 2011;50:4412–9. https://doi.org/10.1021/ie1022628.

[11]   Viteri F, López A, Ángela Millera, Rafael Bilbao, Alzueta M. Influence of temperature and gas

        residence time on the formation of polycyclic aromatic hydrocarbons (PAH) during the pyrolysis of

        ethanol. Fuel 2019;236:820–8. https://doi.org/10.1016/j.fuel.2018.09.061.

[12]   Esarte C, Millera Á, Bilbao R, Alzueta MU. Gas and soot products formed in the pyrolysis of acetylene-

        ethanol blends under flow reactor conditions. Fuel Process Technol 2009;90:496–503.

        https://doi.org/10.1016/j.fuproc.2009.01.011.

[13]   Esarte C, Abián M, Millera Á, Bilbao R, Alzueta MU. Gas and soot products formed in the pyrolysis of

        acetylene mixed with methanol , ethanol , isopropanol or n-butanol. Energy 2012;43:37–46.

        https://doi.org/10.1016/j.energy.2011.11.027.

[14]   McEnally CS, Pfefferle LD. The effects of dimethyl ether and ethanol on benzene and soot formation in

        ethylene nonpremixed flames. Proc Combust Inst 2007;31 I:603–10.

        https://doi.org/10.1016/j.proci.2006.07.005.

[15]   Wu J, Song KH, Litzinger T, Lee SY, Santoro R, Linevsky M, et al. Reduction of PAH and soot in

        premixed ethylene-air flames by addition of ethanol. Combust Flame 2006;144:675–87.

https://doi.org/10.1016/j.combustflame.2005.08.036.

[16] Böhm H, Braun-Unkhoff M. Numerical study of the effect of oxygenated blending compounds on soot formation in shock tubes. Combust Flame 2008;153:84–96. https://doi.org/10.1016/j.combustflame.2008.01.002.

[17] Norton TS, Dryer FL. The flow reactor oxidation of C1-C4 alcohols and MTBE. Symp Combust 1990;23:179–85. https://doi.org/10.1016/S0082-0784(06)80257-2.

[18] Inal F, Senkan SM. Effects of oxygenate additives on polycyclic aromatic hydrocarbons (PAHs) and soot formation. Combust Sci Technol 2002;174:1–19. https://doi.org/10.1080/00102200290021353.

[19] Li W, Zhang Y, Mei B, Li Y, Cao C, Zou J, et al. Experimental and kinetic modeling study of n-propanol and i-propanol combustion: Flow reactor pyrolysis and laminar flame propagation. Combust Flame 2019;207:171–85. https://doi.org/10.1016/j.combustflame.2019.05.040.

[20] Wang R, Cadman P. Soot and PAH Production from Spray Combustion of Different Hydrocarbons Behind reflected Shock Waves. Combust Flame 1998;112:359–70. https://doi.org/10.1016/S0010-2180(97)00134-X.

[21] Moss JT, Berkowitz AM, Oehlschlaeger MA, Biet J, Warth V, Glaude PA, et al. An experimental and kinetic modeling study of the oxidation of the four isomers of butanol. J Phys Chem A 2008;112:10843–55. https://doi.org/10.1021/jp806464p.

[22] Johnson M V., Goldsborough SS, Serinyel Z, O'Toole P, Larkin E, O'Malley G, et al. A shock tube study of n- and iso-propanol ignition. Energy and Fuels 2009;23:5886–98. https://doi.org/10.1021/ef900726j.

[23] Heufer KA, Fernandes RX, Olivier H, Beeckmann J, Röhl O, Peters N. Shock tube investigations of ignition delays of n-butanol at elevated pressures between 770 and 1250 K. Proc Combust Inst 2011;33:359–66. https://doi.org/10.1016/j.proci.2010.06.052.

[24] Stranic I, Chase DP, Harmon JT, Yang S, Davidson DF, Hanson RK. Shock tube measurements of ignition delay times for the butanol isomers. Combust Flame 2012;159:516–27. https://doi.org/10.1016/j.combustflame.2011.08.014.

[25] Yang K, Zhan C, Man X, Guan L, Huang Z, Tang C. Shock Tube Study on Propanal Ignition and the Comparison to Propane, n-Propanol, and i-Propanol. Energy and Fuels 2016;30:717–24. https://doi.org/10.1021/acs.energyfuels.5b02739.

[26] Charles S. M, Lisa D. P. Fuel decomposition and hydrocarbon growth processes for oxygenated

hydrocarbons: Butyl alcohols. Proc Combust Inst 2005;30:1363–70.

https://doi.org/10.1016/j.proci.2004.07.033.

[27]   Yang B, Oßwald P, Li Y, Wang J, Wei L, Tian Z, et al. Identification of combustion intermediates in

isomeric fuel-rich premixed butanol-oxygen flames at low pressure. Combust Flame 2007;148:198–209.

https://doi.org/10.1016/j.combustflame.2006.12.001.

[28]   Li YY, Wei LX, Tian Z, Yang B, Wang J, Zhang TC, et al. A comprehensive experimental study of

low-pressure premixed C3-oxygenated hydrocarbon flames with tunable synchrotron photoionization.

Combust Flame 2008;152:336–59. https://doi.org/10.1016/j.combustflame.2007.10.012.

[29]   Kasper T, Kohse-Höinghaus K, Taatjes CA, Oßwald P, Law ME, Wang J, et al. Combustion chemistry

of the propanol isomers — investigated by electron ionization and VUV-photoionization molecular-

beam mass spectrometry. Combust Flame 2009;156:1181–201.

https://doi.org/10.1016/j.combustflame.2009.01.023.

[30]   Frassoldati A, Cuoci A, Faravelli T, Niemann U, Ranzi E, Seiser R, et al. An experimental and kinetic

modeling study of n-propanol and iso-propanol combustion. Combust Flame 2010;157:2–16.

https://doi.org/10.1016/j.combustflame.2009.09.002.

[31]   Hansen N, Harper MR, Green WH. High-temperature oxidation chemistry of n-butanol - Experiments in

low-pressure premixed flames and detailed kinetic modeling. Phys Chem Chem Phys 2011;13:20262–

74. https://doi.org/10.1039/c1cp21663e.

[32]   Camacho J, Lieb S, Wang H. Evolution of size distribution of nascent soot in n- and i-butanol flames.

Proc Combust Inst 2013;34:1853–60. https://doi.org/10.1016/j.proci.2012.05.100.

[33]   Singh P, Sung C. PAH formation in counterflow non-premixed flames of butane and butanol isomers.

Combust Flame 2016;170:91–110. https://doi.org/10.1016/j.combustflame.2016.05.009.

[34]   Lü X, Hou Y, Ji L, Zu L, Huang Z. Heat release analysis on combustion and parametric study on

emissions of HCCI engines fueled with 2-propanol/n-heptane blend fuels. Energy and Fuels

2006;20:1870–8. https://doi.org/10.1021/ef0601263.

[35]   Zervas E, Montagne X, Lahaye J. Emission of alcohols and carbonyl compounds from a spark ignition

engine. Influence of fuel and air/fuel equivalence ratio. Environ Sci Technol 2002;36:2414–21.

https://doi.org/10.1021/es010265t.

[36]   Popuri SSS, Bata RM. A performance study of iso-butanol-, methanol-, and ethanol-gasoline blends

using a single cylinder engine. SAE Tech Pap 1993;102:576–95. https://doi.org/10.4271/932953.

[37] Rakopoulos DC, Rakopoulos CD, Hountalas DT, Kakaras EC, Giakoumis EG, Papagiannakis RG. Investigation of the performance and emissions of bus engine operating on butanol/diesel fuel blends. Fuel 2010;89:2781–90. https://doi.org/10.1016/j.fuel.2010.03.047.

[38] Yao M, Wang H, Zheng Z, Yue Y. Experimental study of n-butanol additive and multi-injection on HD diesel engine performance and emissions. Fuel 2010;89:2191–201. https://doi.org/10.1016/j.fuel.2010.04.008.

[39] Viteri F, Gracia S, Millera Á, Bilbao R, Alzueta MU. Polycyclic aromatic hydrocarbons (PAHs) and soot formation in the pyrolysis of the butanol isomers. Fuel 2017;197:348–58. https://doi.org/10.1016/j.fuel.2017.02.026.

[40] Vikeri F, Gracia S, Ángela Millera, Rafael Bilbao, Maria Alzueta. Polycyclic aromatic hydrocarbons (PAHs) and soot formation in the pyrolysis of the butanol isomers. Fuel 2017;197:348–58. https://doi.org/10.1016/j.fuel.2017.02.026.

[41] Schoeny R, Poirier K. Provisional guidance for quantitative risk assessment of polycyclic aromatic hydrocarbons. US Environmental Protection Agency, Office of Research and Development, Office of Health and Environmental Assessment, Washington DC (NTIS PB94116571). 1993. https://doi.org/EPA/600/R-93/089.

[42] Ian N, Peter L. Toxic Equivalency Factors (TEFs) for Polycyclic Aromatic Hydrocarbons (PAHs). Regul Toxicol Pharmacol 1992;16:290–300. https://doi.org/10.1016/0273-2300(92)90009-X.

[43] Inal F, Senkan SM. Effects of oxygenate additives on polycyclic aromatic hydrocarbons (PAHs) and soot formation. Combust Sci Technol 2002;174:1–19. https://doi.org/10.1080/00102200290021353.

[44] Wang H, Frenklach M. A detailed kinetic modeling study of aromatics formation in laminar premixed acetylene and ethylene flames. Combust Flame 1997;110:173–221. https://doi.org/10.1016/S0010-2180(97)00068-0.

[45] Dandajeh HA, Ladommatos N, Hellier P, Eveleigh A. Effects of unsaturation of C2and C3hydrocarbons on the formation of PAHs and on the toxicity of soot particles. Fuel 2017;194:306–20. https://doi.org/10.1016/j.fuel.2017.01.015.

[46] Dandajeh HA, Ladommatos N, Hellier P, Eveleigh A. In fluence of carbon number of C 1 – C 7 hydrocarbons on PAH formation. Fuel 2018;228:140–51. https://doi.org/10.1016/j.fuel.2018.04.133.

[47] Eveleigh A, Ladommatos N, Balachandran R, Marca A. Conversion of oxygenated and hydrocarbon molecules to particulate matter using stable isotopes as tracers. Combust Flame 2014;161:2966–74.

https://doi.org/10.1016/j.combustflame.2014.05.008.

[48]   Eveleigh A, Ladommatos N, Hellier P, Jourdan A. An investigation into the conversion of specific carbon atoms in oleic acid and methyl oleate to particulate matter in a diesel engine and tube reactor. Fuel 2015;153:604–11. https://doi.org/10.1016/j.fuel.2015.03.037.

[49]   Eveleigh A. The influence of fuel molecular structure on particulate emission investigated with isotope tracing. University College London, 2015.

[50]   Oukebdane K, Portet-koltalo F, Machour N, Dionnet F, Desbène PL. Talanta Comparison of hot Soxhlet and accelerated solvent extractions with microwave and supercritical fluid extractions for the determination of polycyclic aromatic hydrocarbons and nitrated derivatives strongly adsorbed on soot collected inside a diesel. Talanta 2010;82:227–36. https://doi.org/10.1016/j.talanta.2010.04.027.

[51]   Yacoub Y, Bata R, Gautam M. The performance and emission characteristics of C1-C5 alcohol-gasoline blends with matched oxygen content in a single-cylinder spark ignition engine. Proc Inst Mech Eng Part A J Power Energy 1998;212:363–79. https://doi.org/10.1243/0957650981536934.

[52]   Dean JA. Lange's Handbook of Chemistry, 14th edition. McGraw-Hill, New York; 1992.

[53]   Sarathy SM, Oßwald P, Hansen N, Kohse-Höinghaus K. Alcohol combustion chemistry. Prog Energy Combust Sci 2014;44:40–102. https://doi.org/10.1016/j.pecs.2014.04.003.

[54]   Dandajeh HA. Effect of molecular structure of liquid and gaseous fuels on the formation and emission of PAHs and soot. University College London, 2017.

[55]   Veloo PS, Egolfopoulos FN. Studies of n-propanol, iso-propanol, and propane flames. Combust Flame 2011;158:501–10. https://doi.org/10.1016/j.combustflame.2010.10.001.

[56]   Miller JA, Melius CF. Kinetic and Thermodynamic Issues in the Formation of Aromatic Compounds in Flames of Aliphatic Fuels. Combust Flame 1992;91:21–39. https://doi.org/10.1016/0010-2180(92)90124-8.

[57]   Hansen N, Braun-Unkhoff M, Kathrotia T, Lucassen A, Yang B. Understanding the reaction pathways in premixed flames fueled by blends of 1,3-butadiene and n-butanol. Proc Combust Inst 2015;35:771–8. https://doi.org/10.1016/j.proci.2014.05.005.

[58]   Colket MB, Seery DJ. REACTION MECHANISMS FOR TOLUENE PYROLYSIS. Twenty-Fifth Symp. Combust. Combust. Inst., 1994, p. 883–91. https://doi.org/10.1016/S0082-0784(06)80723-X.

[59]   Appel J, Bockhorn H, Frenklach M. Kinetic modeling of soot formation with detailed chemistry and physics: Laminar premixed flames of C2 hydrocarbons. Combust Flame 2000;121:122–36.

https://doi.org/10.1016/S0010-2180(99)00135-2.

[60]   Dandajeh HA, Ladommatos N, Hellier P, Eveleigh A. Effects of unsaturation of C2 and C3
         hydrocarbons on the formation of PAHs and on the toxicity of soot particles. Fuel 2017;194:306–20.
         https://doi.org/10.1016/j.fuel.2017.01.015.

[61]   Cole JA, Bittner JD, Longwell JP, Howard JB. Formation Mechanisms of Aromatic Compounds in
         Aiiphatic Flames. Combust Flame 1984;56:51–70. https://doi.org/10.1016/0010-2180(84)90005-1.

[62]   Frenklach M, Clary DW, Gardiner WC, Stein SE. Detailed kinetic modeling of soot formation in shock-
         tube pyrolysis of acetylene. Symp Combust 1984;20:887–901. https://doi.org/10.1016/S0082-
         0784(85)80578-6.

[63]   Frenklach M. Reaction mechanism of soot formation in flames. Phys. Chem. Chem. Phys., vol. 4, 2002,
         p. 2028–37. https://doi.org/10.1039/b110045a.

[64]   Justi R. TEACHING AND LEARNING CHEMICAL KINETICS. In: Gilbert JK, Jong O De, Justi R,
         Treagust DF, Driel JH Van, editors. Chem. Educ. Towar. Res. Pract., vol. 17, Springer; 2013, p. 293–
         315. https://doi.org/10.1007/0-306-47977-X_13.

[65]   Liu P, Li Z, Bennett A, Lin H, Sarathy SM, Roberts WL. The site effect on PAHs formation in HACA-
         based mass growth process. Combust Flame 2019;199:54–68.
         https://doi.org/10.1016/j.combustflame.2018.10.010.

[66]   Mathieu O, Frache G, Djebaïli-Chaumeix N, Paillard CE, Krier G, Muller JF, et al. Characterization of
         adsorbed species on soot formed behind reflected shock waves. Proc Combust Inst 2007;31 I:511–9.
         https://doi.org/10.1016/j.proci.2006.07.190.

[67]   Ruiz MP, Callejas A, Millera A, Alzueta MU, Bilbao R. Soot formation from C2H2 and C2H4 pyrolysis
         at different temperatures. J Anal Appl Pyrolysis 2007;79:244–51.
         https://doi.org/10.1016/j.jaap.2006.10.012.

[68]   Eveleigh A, Ladommatos N, Hellier P, Jourdan AL. Quantification of the Fraction of Particulate Matter
         Derived from a Range of 13C-Labeled Fuels Blended into Heptane, Studied in a Diesel Engine and
         Tube Reactor. Energy and Fuels 2016;30:7678–90. https://doi.org/10.1021/acs.energyfuels.6b00322.

[69]   Westbrook CK, Pitz WJ, Curran HJ. Chemical kinetic modeling study of the effects of oxygenated
         hydrocarbons on soot emissions from diesel engines. J Phys Chem A 2006;110:6912–22.
         https://doi.org/10.1021/jp056362g.

[70]   Rotzoll G. High-temperature pyrolysis of ethanol. J Anal Appl Pyrolysis 1985;9:43–52.

https://doi.org/10.1016/0165-2370(85)80005-X.

[71]   Curran HJ, Fisher EM, Glaude PA, Marinov NM, Pitz WJ, Westbrook CK, et al. Detailed chemical

          kinetic modeling of diesel combustion with oxygenated fuels. SAE Tech Pap 2001;110.

          https://doi.org/10.4271/2001-01-0653.

[72]   Sharma RK, Hajaligol MR. Effect of pyrolysis conditions on the formation of polycyclic aromatic

          hydrocarbons (PAHs) from polyphenolic compounds. J Anal Appl Pyrolysis 2003;66:123–44.

          https://doi.org/10.1016/S0165-2370(02)00109-2.

[73]   Bittner JD, Howard JB. Composition profiles and reaction mechanisms in a near-sooting premixed

          benzene/oxygen/argon flame. Symp Combust 1981;18:1105–16.

          https://doi.org/https://doi.org/10.1016/S0082-0784(81)80115-4.

[74]   Kislov V V, Sadovnikov AI, Mebel AM. Formation Mechanism of Polycyclic Aromatic Hydrocarbons

          beyond the Second Aromatic Ring. J Phys Chem 2013;117:4794–816.

          https://doi.org/https://doi.org/10.1021/jp402481y.

[75]   Shukla B, Koshi M. A novel route for PAH growth in HACA based mechanisms. Combust Flame

          2012;159:3589–96. https://doi.org/10.1016/j.combustflame.2012.08.007.

[76]   Shukla B, Koshi M. Comparative study on the growth mechanisms of PAHs. Combust Flame

          2011;158:369–75. https://doi.org/10.1016/j.combustflame.2010.09.012.